

MICROMECHANICS IN CONTINUOUS GRAPHITE FIBER/EPOXY COMPOSITES DURING CREEP

C.H. Zhou¹, I. J. Beyerlein², and L. S. Schadler¹

¹Materials Science and Engineering, Rensselaer Polytechnic Institute
Troy, NY12180, USA

²Los Alamos National Laboratory, Los Alamos, MS G755, NM 87545, USA.

ABSTRACT: Micro Raman spectroscopy and classic composite shear-lag models were used to analyze the evolution with time of fiber and matrix strain/stress around fiber breaks in planar model graphite fiber-epoxy matrix composites. Impressive agreements were found between the model predictions and the experimental results. The local matrix creep leads to an increase in the load transfer length around the break under a constant load. This increases the chance of fiber breakage in the neighboring intact fibers.

KEYWORDS: Micromechanics, polymer composites, creep, Raman spectroscopy, modeling

1. INTRODUCTION

An important issue in the design of polymer composite structures is prediction of their time dependent performance and lifetime. The macroscopic failure of polymer composites is believed to start from localized damage zones (fiber breaks, matrix cracks, etc.), which inevitably form during fabrication or initial loading. Under a constant load, these initially harmless damage zones may grow in time and interact with each other, due to the time dependent nature of the polymer matrix. When one of these damage zones grows beyond a critical size, final failure of the structure takes place without any visible warning. Because failure of the composite is the result of a series of micro-events, a powerful experimental tool is required to investigate the creep-failure process at the micro scale, instead of the traditional macro-scale tests, in order to build an effective lifetime-predicting model.

In recent years, micro Raman spectroscopy (MRS) has been used to directly measure the axial strain along the fibers in composites [1-3]. Since many high performance fibers have great Raman sensitivity to strain, no other technique is comparable to MRS in strain measurements at micro scale in fiber-reinforced composites. However, most work in this area has been done on the time independent response. In this work, micro Raman spectroscopy was used to investigate the strain/stress evolution along a broken fiber in multi-fiber model composites during creep at room temperature. Predictions from a viscous break interaction (VBI) model [4] based on classic shear-lag concepts were compared with the experimental data.

2. VISCOUS BREAK INTERACTION (VBI) MODEL

VBI is a shear-lag analysis for a multi-fiber composite. The details of the 2D version used here can be found in Beyerlein et al. [4]. Figure 1 shows a region in a composite lamina of evenly spaced fibers and matrix regions and containing a couple of fiber breaks. As indicated, E is the fiber Young's modulus, w is the inter-fiber spacing (surface-to-surface), d is the fiber diameter, A is the fiber cross-sectional area, and b is the out-

of-plane thickness of the model. Here b is set equal to d . In the fiber axial direction x , a constant far field strain per fiber, denoted ε^* , is applied.

The time dependent compliance of the matrix $J(\mathcal{T})$ is well described with a common three parameter expression we term the “complete power law” compliance model, which is

$$J(\mathcal{T}) = J_1 [1+(\mathcal{T}/\mathcal{T}_c)^\alpha] \quad (1a)$$

where \mathcal{T} is time, \mathcal{T}_c is the relaxation time, α is the power law exponent and J_1 is the initial compliance. For long times, i.e. $\mathcal{T} \rightarrow \infty$, $J(\mathcal{T})$, apart from the initial elastic response, can also be well represented using the following “incomplete power law” function in time, where J_e is a compliance constant,

$$J(\mathcal{T}) = J_e(\mathcal{T}/\mathcal{T}_c)^\alpha \quad (1b)$$

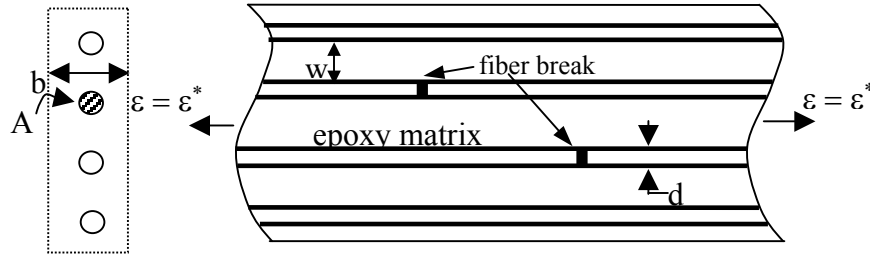


Figure 1: Illustration of the geometry of the 2-D array of fibers used in the VBI model

Consider an isolated fiber break in a 2D lamina (see Figure 1) with a matrix viscoelastic compliance following the power law function (Eqn.1b). Let $\varepsilon_r^* = \varepsilon_r/\varepsilon^*$ be the constant residual axial strain in the fiber normalized by the far field fiber strain ε^* . According to the model [4], the axial fiber strain $\varepsilon_0(z)$ along a fiber with a break at $x = 0$ is,

$$\varepsilon_0(z)/\varepsilon^* \approx 1 - \frac{(1 - \varepsilon_r^*)}{2} C_\theta [\exp\{-2C_\theta \beta_0 |z|\}] d\theta - \kappa_1(\alpha) |z| \int_0^\pi C_\theta^2 [\exp\{-2C_\theta \beta_0 |z|\}] d\theta, \quad (2)$$

where $C_\theta = \sin(\theta/2)$, $z = (x/\delta)/(\mathcal{T}/\mathcal{T}_c)^{\alpha/2}$, $\delta = \sqrt{E A w J_e / d}$, and

$$\beta_0 = \Gamma(1+\alpha/2)/\sqrt{\Gamma(1+\alpha)}, \quad \kappa_1(\alpha) = \frac{(\pi\alpha/2)^2}{6} \beta_0 \quad (3)$$

Use of Eqn.1b for $J(\mathcal{T})$ not only simplifies the analysis such that we are able to obtain the closed form result but the fiber strain depends only on the parameter $z = (x/\delta)(\mathcal{T}_c/\mathcal{T})^{\alpha/2}$, which couples space and time. Similarly for $\varepsilon_1(z)$, the axial strain in the intact fibers adjacent to the break at $x = 0$, the model predicts

$$\varepsilon_1(z)/\varepsilon^* \approx 1 - \frac{(1 - \varepsilon_r^*)}{2} \int_0^\pi \cos(\theta) C_\theta [\exp\{-2C_\theta \beta_0 |z|\}] d\theta - \kappa_1(\alpha) |z| \int_0^\pi \cos(\theta) C_\theta^2 \exp\{-2C_\theta \beta_0 |z|\} d\theta, \quad (4)$$

3. EXPERIMENTAL DETAILS

Figure 2 shows the geometry of the model fiber composite specimens fabricated for this MRS (micro Raman spectroscopy) experiment. The matrix is an epoxy (Epon 828+ Epi-Cure 3234 curing agent at 1:0.129 ratio) with a modulus of 3.3 GPa, a shear modulus of 1.26 GPa and a Poisson’s ratio of 0.33. The fiber is a Toray M40 high modulus graphite fiber with an axial modulus of $E=390$ GPa, a shear modulus of 147 GPa, and an average fiber diameter of 6.6 μm . A planar array of 5~8 fibers was placed with relatively uniform spacing in the middle of the dog-bone shaped mold. Bordering this fiber array were graphite fiber tows to reduce the macroscopic creep during the test. The composite samples were cured at room temperature for 12 hrs and post-cured at 100°C for 2 hrs.

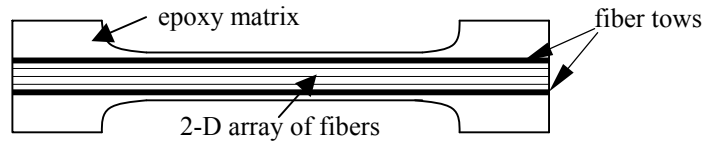


Figure 2: Schematic showing the geometry of the model composites

A constant uniform load was applied to the samples using custom-built jigs. A strain gauge was attached directly to the sample surface to monitor the macro-strain. Load was applied until a break was observed in a fiber and was then held constant. The macroscopic creep was negligible during the test period. Raman spectra were recorded along the broken fiber at periodic time intervals for several weeks, using a Renishaw Ramanscope System 2000, and a 514 nm Argon ion laser which has a spatial resolution of approximately $\pm 1 \mu\text{m}$. The strain in the fibers was calculated from the shift in the second order A_{1g} mode. From the fiber strain data, the interfacial shear stress (ISS) was calculated using a simple force balance

$$ISS = E (d/4) d\varepsilon/dx \quad (5)$$

4. RESULTS AND DISCUSSION

4.1 Bulk Matrix Creep Tests

In order to obtain the time dependent response of the matrix, long-term creep tests (~ 20 days) were performed on the bulk epoxy matrix. Figure 3 shows the change in matrix shear compliance with time at room temperature for the bulk epoxy at two different stress levels (10MPa and 20MPa). The power law functions (Eqn.1a) and (Eqn.1b) were used to fit the data. As shown in Figure 3, Eqn.1a provides a good description of the data, while Eqn.1b can only be used to describe the long-term behavior.

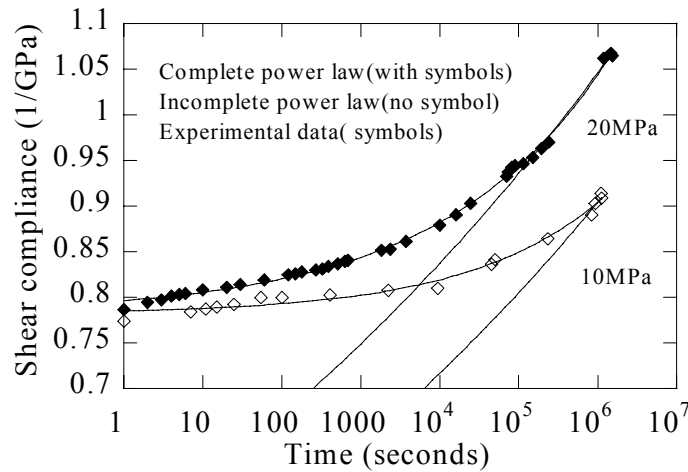


Figure 3: A plot of creep compliance $J(t)$ versus time of the bulk matrix

TABLE 1
COMPARISON OF THE PARAMETERS ASSOCIATED WITH DIFFERENT CREEP FUNCTIONS
FOR THE EPOXY MATRIX

Parameters	Compliance constant J_1 , or J_e , (1/GPa)		Relaxation time τ_c (seconds)		Shape parameter α	
	10	20	10	20	10	20
Complete Power Law $J(t) = J_1 + J_1(t/\tau_c)^\alpha$	0.78	0.78	1.4×10^9	1.9×10^8	0.26	0.21
Incomplete Power Law $J(t) = J_e(t/\tau_c)^\alpha$	0.93	1.03	1.7×10^6	7×10^5	0.05	0.048

Table 1 lists the values for the parameters associated with these two different functions. The shape parameter α did not change significantly with the stress level, especially for the incomplete power law. However, for both laws, the relaxation time \mathcal{T}_C tends to decrease with increasing applied stress.

4.2 MRS Data and Model Predictions for Multi-fiber Composite

In this section, the measured axial strain distributions and the calculated interfacial stress (ISS) at different times are compared with VBI model predictions using parameters from Eqn.1a or Eqn.1b, as listed in Table.1. In one of our multi-fiber model samples, two fibers were very close to each other with an inter-fiber spacing of $13\mu\text{m}$. A break was found in one fiber when the applied macroscopic strain was 1%. Figure 4 shows the strain along the two fibers with model predictions at two different times, $\tau = 3.6 \times 10^4$ and $\tau = 2.5 \times 10^6$ seconds after the fiber broke.

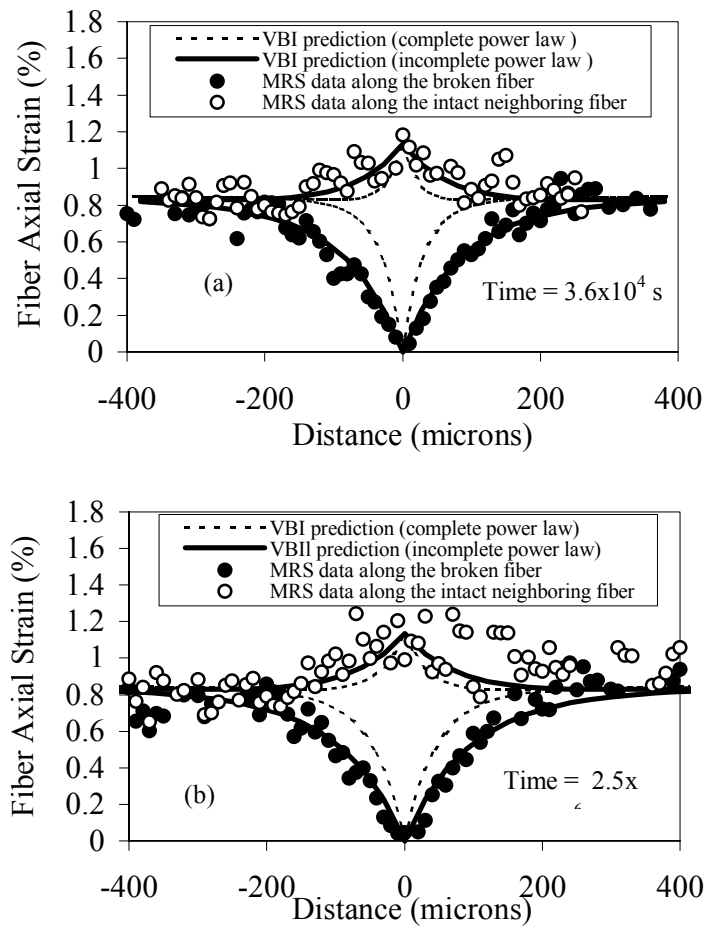


Figure 4: A comparison of the experimental axial strain data and the model predictions using complete power law parameters or incomplete power law parameters at 1% macrostrain at (a) 3.6×10^4 s; (b) 2.5×10^6 s

The VBI model predictions using incomplete power law parameters are in very good agreement with the experimental data, while the predictions with complete power law parameters only give qualitative descriptions of the strain profiles. This is not surprising because the model solutions are derived using the incomplete power law function for the matrix shear creep compliance. In fact, the parameters from both stress levels (10MPa and 20MPa) were used to calculate the strain distributions. It was found that the predictions were almost identical for the two sets of parameters despite the difference in \mathcal{T}_C . An important feature in Figure 4 is the scattering of the axial strain data along the neighboring intact fiber. As described in Beyerlein’s work [5], a fiber break will produce a stress concentration along the nearby fibers. In the ideal elastic case, the stress concentration appears as a sharp peak located at the fiber break. This peak would be

obscured and broadened if there is any matrix yielding or interfacial debonding near the break. Figure 4 suggests the presence of inelastic zones near the fiber break and possible growth of the inelastic zone during the creep.

In Figure 5 and Figure 6, only predictions from the incomplete power law are compared with the MRS results. The interfacial shear stress (ISS) distributions along the right part of the broken fiber are illustrated in Figure 5. The feature of the experimentally derived ISS curve at 3.6×10^4 seconds suggests some local matrix yielding might have occurred near the fiber break. As defined by Beyerlein et al [6], the load recovery length is the distance between the ISS_{max} (usually located at the fiber end) and the point where the ISS asymptotically approaches zero. The ISS profiles from MRS data show an increase of the load recovery length, while the peak value for the ISS did not change much over the time period. For the neighboring intact fiber, we define the positively affected length as the distance between the two points where the ISS approaches zero symmetric to the break. Corresponding to the increase in the load transfer length in Figure 5, the positively affected length in the intact neighboring fiber also expanded in time, as shown in Figure 6. This increases the chance of failure in the neighboring fiber, as was observed in this sample when a break occurred in the neighboring fiber at $112 \mu\text{m}$ from the original break after 3×10^6 seconds. Although the model also predicts a similar increase in the load recovery length, the predicted change is smaller than that shown from the experimental results.

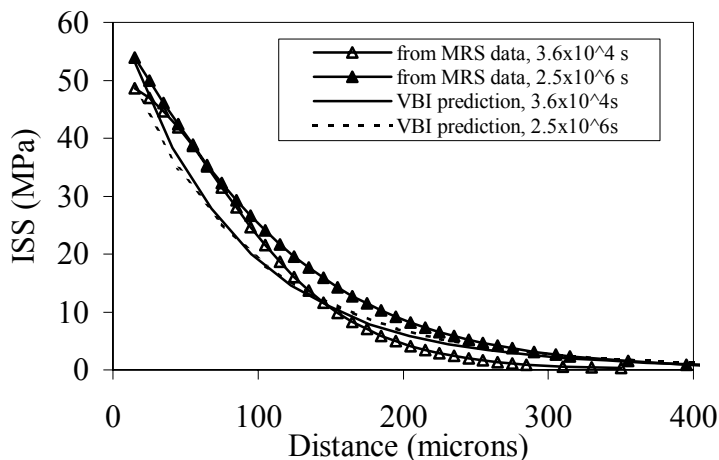


Figure 5: A comparison of the ISS derived from the experimental data and the model predictions using incomplete power law parameters at 1% macrostrain for the right part of the broken fiber at two different times

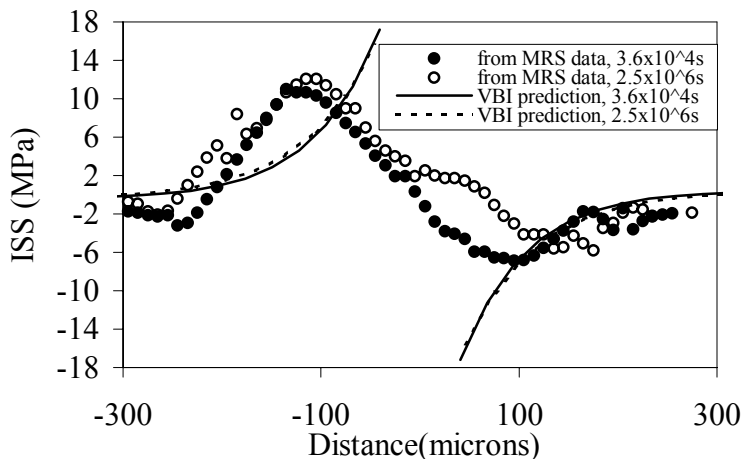


Figure 6: A comparison of the experimentally derived ISS and the model predictions using incomplete power law parameters for the intact neighboring fiber at two different times

For this composite sample, the solutions using the complete power law parameters did not show very good agreement with the MRS results. Although the incomplete law (Eqn.1b) works well only for the long-term creep of the polymer matrix, the VBI predictions using its parameters show excellent agreement with the MRS data, especially the axial strain profiles along the broken fiber. The smaller change in the predicted ISS profiles might partly result from the difference between the idealized model and the real composite sample. In the sample the fibers were not strictly evenly spaced. Two fibers were 13 μm apart, while other fibers were 25~30 μm away from them. Since the model considers evenly spaced fibers, it is very likely that the model predicts changes smaller than that in the real sample where the local matrix volume fraction is higher. As described in the previous section, this model does not include the possible plastic deformation and the interfacial debonding near the fiber break. For graphite reinforced epoxy composites, interfacial debonding or matrix yielding is common near the fiber break at relatively high strains. Therefore, it will be necessary to take into account these non-linear phenomena in future models.

5. CONCLUSIONS

The stress/strain redistribution during the creep of graphite fiber reinforced epoxy composites was investigated experimentally with Micro Raman spectroscopy and theoretically with a simple but effective viscoelastic shear lag model using VBI technique. Model predictions using the incomplete power law for the matrix creep showed good agreement with the experimental results. It was confirmed that the load transfer length increased due to the local matrix creep near fiber breaks under a constant load. This can explain why new fiber fractures occur later in time and are usually offset from the plane of the original break.

REFERENCE:

1. Melanitis, N., Galiotis, C., Tetlow, P.L. and Davies, K.L. (1993) *J.Mater. Sci.*, **28**, 1648
2. Schadler, L. S. and Galiotis, C. (1995) *Int.l Mater. Rev.*, **40**, 116
3. Thomsen J.S. and Pyrz R. (2000) *Compos. Sci. Technol.* **60**, 1791
4. Beyerlein, I.J., Phoenix, S.L. & Raj, R. (1998) *Int. J. Solids Strucutres* **35**, 3177
5. Beyerlein, I. J., Amer, M., Schadler, L. S. and Phoenix, S. L. (1998) *Sci. Eng.Compos. Mater.*, **7**, 151
6. Beyerlein, I. J., Zhou, C. H., and Schadler, L. S. (2001) Proceedings of the ICOSAR conference, June 2001, New Port Beach, California.